

Synthesis and Photophysical Properties of Trimetallic Acetylide Complexes with a 1,3,5-Triazine Core

Quan Yuan Hu,[†] Wei Xin Lu,[‡] Hong Ding Tang,[†] Herman H. Y. Sung,[†] Ting Bin Wen,[†] Ian D. Williams,[†] George K. L. Wong,^{*,‡} Zhenyang Lin,^{*,†} and Guochen Jia^{*,†}

Department of Chemistry and Open Laboratory of Chirotechnology of the Institute of Molecular Technology for Drug Discovery and Synthesis and Department of Physics, The Hong Kong University of Science and Technology, Clear Water Bay, Kowloon, Hong Kong

Received March 20, 2005

Treatment of 2,4,6-tris(4-bromophenyl)-1,3,5-triazine (2,4,6-(4-BrC₆H₄)₃-1,3,5-C₃N₃) with HC≡CSiMe₃ in the presence of Pd(PPh₃)₄/CuI and NEt₃ produces 2,4,6-[4-(Me₃SiC≡C)C₆H₄]₃-1,3,5-C₃N₃, which reacts with Bu₄NF to yield 2,4,6-[4-(HC≡C)C₆H₄]₃-1,3,5-C₃N₃. Reaction of 2,4,6-[4-(HC≡C)C₆H₄]₃-1,3,5-C₃N₃ with AuCl(PPh₃) in the presence of NEt₃ produces the gold acetylide complex 2,4,6-[4-(PPh₃)AuC≡C]C₆H₄]₃-1,3,5-C₃N₃. Treatment of 2,4,6-[4-(HC≡C)C₆H₄]₃-1,3,5-C₃N₃ with *cis*-RuCl₂(dppe)₂/NaPF₆ followed by NEt₃ gives 2,4,6-[4-(Cl(dppe)₂RuC≡C)C₆H₄]₃-1,3,5-C₃N₃, which reacts with *p*-HC≡CC₆H₄R (R = OCH₃, NO₂) to give 2,4,6-[4-(4-RC₆H₄C≡C)(dppe)₂RuC≡C]C₆H₄]₃-1,3,5-C₃N₃. The electrochemical and photophysical properties of the new complexes have been investigated.

Introduction

There has been considerable interest in the synthesis and properties of hyperbranched and dendritic organometallic compounds with metal–acetylide linkages.¹ A number of trimetallic acetylide complexes with a 1,3,5-substituted benzene core have been synthesized in recent years,^{2–16} including 1,3,5-[L_nMC≡C]₃C₆H₃ (M = Fe,² Ru,³ Rh,⁹ Ir,¹⁰ Pd,^{11,12} Pt,^{12–14} Au^{15,16}) and 1,3,5-

[L_nMC≡CC₆H₄C≡C]₃C₆H₃ (M = Ru,^{5,6} Os⁸). Interesting physical properties have been reported for some of these complexes. For example, complexes such as 1,3,5-[Cl(PET₃)₂MC≡CC₆H₄C≡C]₃C₆H₃ (M = Pd, Pt) exhibit luminescent properties,^{11,12} complexes such as 1,3,5-[PPh₃)AuC≡C]₃C₆H₃,¹⁵ 1,3,5-[Cl(dppe)₂RuC≡CC₆H₄C≡C]₃C₆H₃,^{6a} and 1,3,5-[Cl(dppm)₂RuC≡CC₆H₄CH=CH]₃C₆H₃⁷ have good NLO properties,¹⁷ and complexes such as 1,3,5-[Cp*(dppe)FeC≡C]₃C₆H₃² and [Cp(PPh₃)₂RuC≡C]₃C₆H₃³ show electronic cooperation between individual metal centers.

This work concerns the synthesis and properties of acetylide complexes containing a 1,3,5-triazine core, which is more electron-withdrawing than benzene. Organic compounds of 1,3,5-triazine derivatives have been widely explored for their material properties, such as luminescent,¹⁸ nonlinear optical,¹⁹ and liquid crystalline²⁰ properties. In term of nonlinear optical properties, it has been demonstrated that octupolar organic compounds with a 1,3,5-triazine core could have larger first hyperpolarizability β values than analogous organic compounds with a 1,3,5-benzene core.¹⁹ⁱ Thus, trimetallic acetylide compounds with a 1,3,5-triazine core may

[†] Department of Chemistry and Open Laboratory of Chirotechnology of the Institute of Molecular Technology for Drug Discovery and Synthesis.

[‡] Department of Physics.

(1) Paul, F.; Lapinte, C. *Coord. Rev.* **1998**, 178–180, 431. (b) Long, N. J.; Williams, C. K. *Angew. Chem., Int. Ed.* **2003**, 42, 2586.

(2) (a) Weyland, T.; Ledoux, I.; Brasselet, S.; Zyss, J.; Lapinte, C. *Organometallics* **2000**, 19, 5235. (b) Weyland, T.; Costuas, K.; Toupet, L.; Halet, J. F.; Lapinte, C. *Organometallics* **2000**, 19, 4228. (c) Weyland, T.; Costuas, K.; Mari, A.; Halet, J. F.; Lapinte, C. *Organometallics* **1998**, 17, 5569. (d) Weyland, T.; Lapinte, C.; Frapper, G.; Calhorda, M. J.; Halet, J. F.; Toupet, L. *Organometallics* **1997**, 16, 2024.

(3) Long, N. J.; Martin, A. J.; de Biani, F. F.; Zanello, F. *J. Chem. Soc., Dalton Trans.* **1998**, 2017.

(4) Long, N. J.; Martin, A. J.; White, A. J. P.; Williams, D. J.; Fontani, M.; Laschi, F.; Zanello, P. *Dalton* **2000**, 3387.

(5) Uno, M.; Dixneuf, P. H. *Angew. Chem., Int. Ed.* **1998**, 37, 1714.

(6) (a) McDonagh, A. M.; Humphrey, M. G.; Samoc, M.; Luther-Davies, B.; Houbrechts, S.; Wada, T.; Sasabe, H.; Persoons, A. *J. Am. Chem. Soc.* **1999**, 121, 1405. (b) McDonagh, A. M.; Humphrey, M. G.; Samoc, M.; Luther-Davies, B. *Organometallics* **1999**, 18, 5195. (c) Hurst, S. K.; Cifuentes, M. P.; Humphrey, M. G. *Organometallics* **2002**, 21, 2353. (d) McDonagh, A. M.; Powell, C. E.; Morrall, J. P.; Cifuentes, M. P.; Humphrey, M. G. *Organometallics* **2003**, 22, 1402.

(7) (a) Hurst, S. K.; Humphrey, M. G.; Isoshima, T.; Wostyn, K.; Asselberghs, I.; Clays, K.; Persoons, A.; Samoc, M.; Luther-Davies, B. *Organometallics* **2002**, 21, 2024. (b) Hurst, S. K.; Lucas, N. T.; Humphrey, M. G.; Isoshima, T.; Wostyn, K.; Asselberghs, I.; Clays, K.; Persoons, A.; Samoc, M.; Luther-Davies, B. *Inorg. Chim. Acta* **2003**, 350, 62.

(8) Morrall, J. P.; Powell, C. E.; Stranger, R.; Cifuentes, M. P.; Humphrey, M. G.; Heath, G. A. *J. Organomet. Chem.* **2003**, 670, 248.

(9) Werner, H.; Bachmann, P.; Laubender, M.; Gevert, O. *Eur. J. Inorg. Chem.* **1998**, 1217.

(10) Tykwinski, R. R.; Stang, P. J. *Organometallics* **1994**, 13, 3203.

(11) Yam, V. W. W.; Zhang, L.; Tao, C. H.; Wong, K. M. C.; Cheung, K. K. *Dalton* **2001**, 1111.

(12) Yam, V. W. W.; Tao, C. H.; Zhang, L.; Wong, K. M. C.; Cheung, K. K. *Organometallics* **2001**, 20, 453.

(13) Leininger, S.; Stang, P. J.; Huang, S. *Organometallics* **1998**, 17, 3981.

(14) (a) Ohshiro, N.; Takei, F.; Onitsuka, K.; Takahashi, S. *J. Organomet. Chem.* **1998**, 569, 195. (b) Onitsuka, K.; Fujimoto, M.; Ohshiro, N.; Takahashi, S. *Angew. Chem., Int. Ed.* **1999**, 38, 689.

(15) Whittal, I. R.; Humphrey, M. G.; Houbrechts, S.; Maes, J.; Persoons, A.; Schmid, S.; Hockless, D. C. R. *J. Organomet. Chem.* **1997**, 544, 277.

(16) Irwin, M. J.; Manojlovic-Muir, L.; Muir, K. W.; Puddephatt, R. J.; Yufit, D. S. *Chem. Commun.* **1997**, 219.

(17) (a) Cifuentes, M. P.; Humphrey, M. G. *J. Organomet. Chem.* **2004**, 689, 3968. (b) Powell, C. E.; Humphrey, M. G. *Coord. Chem. Rev.* **2004**, 248, 725 and references therein.

(18) (a) Pang, J.; Tao, Y.; Freiberg, S.; Yang, X. P.; D'Iorio, M.; Wang, S. *J. Mater. Chem.* **2002**, 12, 206. (b) Lupton, J. M.; Hemingway, L. R.; Samuel, I. D. W.; Burn, P. L. *J. Mater. Chem.* **2000**, 10, 867.

also have interesting physical properties. However, trimetallic acetylide compounds with a 1,3,5-triazine core are still unknown, although 1,3,5-triazines functionalized with additional N or S donors have been used to construct supramolecular and luminescent coordination complexes.^{21,22} In this paper, we wish to describe the synthesis, characterization, and photophysical properties of several acetylide complexes of the type 2,4,6-[L_nMC≡CC₆H₄]₃-1,3,5-C₃N₃. A primary objective of this work is to find out how the metal centers may affect the physical properties.

Results and Discussion

Synthesis of Organic Compounds. The starting material 2,4,6-tris(4-bromophenyl)-1,3,5-triazine (**1**) was prepared from 4-bromobenzonitrile according to the method reported by Inoue et al.²³ The compound 2,4,6-[4-(Me₃SiC≡C)C₆H₄]₃-1,3,5-C₃N₃ (**2**)^{20d} was synthesized by the Pd(0)/Cu(I)-catalyzed coupling reaction of **1** with HC≡CSiMe₃, as shown in Scheme 1. Treatment of **2** with Bu₄NF in methanol gave 2,4,6-[4-(HC≡C)C₆H₄]₃-1,3,5-C₃N₃ (**3**).^{20d} The organic compounds have been characterized by NMR spectroscopy and elemental analysis.

Synthesis of Trimetallic Acetylide Compounds. New gold and ruthenium acetylide complexes can be easily synthesized from **3**. Treatment of **3** with AuCl(PPh₃) in the presence of NEt₃ produced the gold acetylide complex **4**. Complex **4** has been characterized

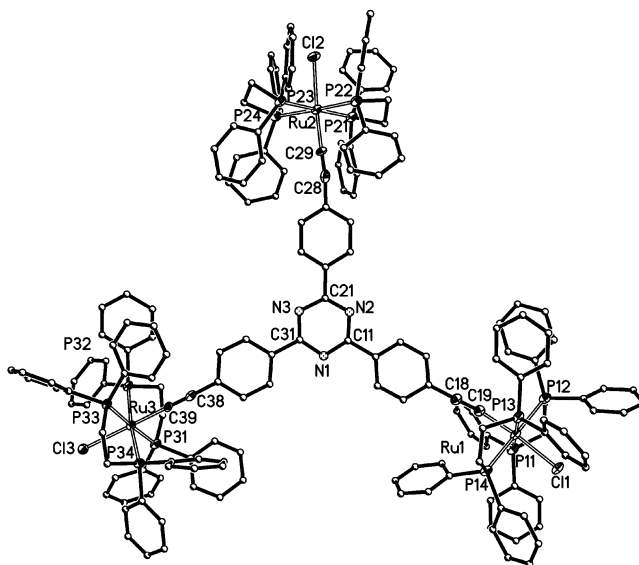


Figure 1. Molecular structure of **5**.

by NMR, IR, and elemental analysis. In particular, the ³¹P{¹H} NMR spectrum (in CD₂Cl₂) showed a singlet at 41.3 ppm, the chemical shift of which is typical of gold acetylides of the type (PPh₃)₃AuC≡CR.²⁴ The presence of the AuC≡C functionality is indicated by the IR spectrum, which showed ν(C≡C) at 2105 cm⁻¹. The related trimetallic gold acetylide complexes 1,3,5-[(PPh₃)₃AuC≡C]₃C₆H₃^{15,16} and 1,3,5-[(PPh₃)₃Au(4-C≡CC₆H₄CH=CH)]₃C₆H₃^{7b} have been reported.

The ruthenium acetylide complex **5** can be prepared by the reaction of 2,4,6-[4-(HC≡C)C₆H₄]₃-1,3,5-C₃N₃ (**3**) with *cis*-RuCl₂(dppf)₂ in the presence of NaPF₆ followed by treatment with NEt₃. The reaction presumably involves deprotonation of the vinylidene intermediate [2,4,6-(4-(Cl(dppf)₂Ru=C=CH)C₆H₄)₃-1,3,5-C₃N₃]³⁺, although we failed to isolate such a complex. The synthetic method was first developed by Dixneuf et al. and has been used previously to prepare ruthenium acetylide complexes such as RuCl(C≡CR)(dppf)₂,²⁵ Cl(dppf)₂RuC≡C₂ArC≡CRu(dppf)₂,²⁶ 1,3,5-[Cl(dppf)₂RuC≡CC₆H₄C≡C]₃C₆H₃,^{5,6a} and 1,3,5-[Cl(dppm)₂RuC≡CC₆H₄-CH=CH]₃C₆H₃.^{7a} Further reactions of **5** with HC≡CC₆H₄R (R = OMe, NO₂) under similar conditions gave the trimetallic complexes **6** and **7**.

Consistent with the structures, the ³¹P{¹H} NMR spectrum of **5** in CD₂Cl₂ showed a singlet at 47.6 ppm, and those of **6** and **7** showed a singlet at ca. 52 ppm. The structure of complex **5** has been confirmed by X-ray diffraction. The molecular structure is shown in Figure 1. The crystallographic details and selected bond distances and angles are given in Tables 1 and 2, respectively. As shown in Figure 1, the compound contains three ruthenium centers linked by a 2,4,6-(C≡CC₆H₄)₃C₃N₃ bridge. The three ruthenium centers

(24) Hunks, W. J.; MacDonald, M. A.; Jennings, M. C.; Puddephatt, R. J. *Organometallics* **2000**, *19*, 5063.

(25) (a) Rigaut, S.; Perruchon, J.; Le Pichon, L.; Touchard, D.; Dixneuf, P. H. *J. Organomet. Chem.* **2003**, *670*, 37. (b) Younus, M.; Long, N. J.; Raithby, P. R.; Lewis, J.; Page, N. A.; White, A. J. P.; Williams, D. J.; Colbert, M. C. B.; Hodge, A. J.; Khan, M. S.; Parker, D. G. *J. Organomet. Chem.* **1999**, *578*, 198. (c) Touchard, D.; Haquette, P.; Guesmi, S.; Le Pichon, L.; Daridor, A.; Toupet, L.; Dixneuf, P. H. *Organometallics* **1997**, *16*, 3640.

(26) Lavastre, O.; Plass, J.; Bachmann, P.; Guesmi, S.; Moinet, C.; Dixneuf, P. H. *Organometallics* **1997**, *16*, 184.

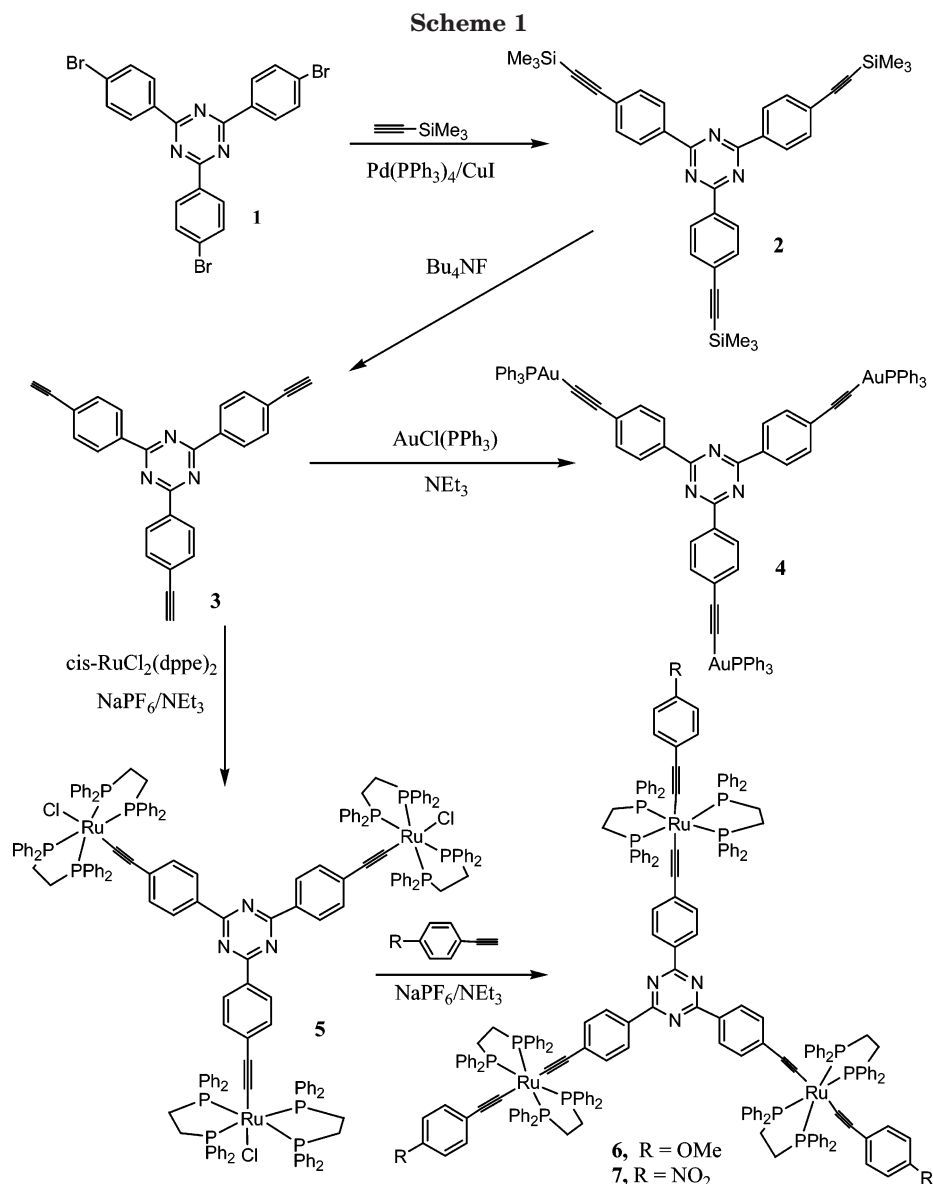
(19) (a) Srinivas, K.; Sitha, S.; Rao, V. J.; Bhanuprakash, K.; Ravikumar, K.; Anthony, S. P.; Radhakrishnan, T. P. *J. Mater. Chem.* **2005**, *15*, 965. (b) Kannan, R.; He, G. S.; Lin, T. C.; Prasad, P. N.; Vaia, R. A.; Tan, L. S. *Chem. Mater.* **2004**, *16*, 185. (c) Cui, Y. Z.; Fang, Q.; Lei, H.; Xue, G.; Yu, W. T. *Chem. Phys. Lett.* **2003**, *377*, 507. (d) Xiang, L.; Liu, Y. G.; Jiang, A. G.; Huang, D. Y. *Chem. Phys. Lett.* **2001**, *338*, 167. (e) Wolf, J. J.; Siegler, F.; Matschiner, R.; Wortmann, R. *Angew. Chem., Int. Ed.* **2000**, *39*, 1436. (f) Thalladi, V. R.; Brasselet, S.; Weiss, H. C.; Blaser, D.; Katz, A. K.; Carrell, H. L.; Boese, R.; Zyss, J.; Nangia, A.; Desiraju, G. R. *J. Am. Chem. Soc.* **1998**, *120*, 2563. (g) Wortmann, R.; Glania, C.; Kramer, P.; Matschiner, R.; Wolff, J. J.; Kraft, S.; Treptow, B.; Barbu, E.; Langle, D.; Gorlitz, G. *Chem. Eur. J.* **1997**, *3*, 1765. (h) Yonehara, H.; Kang, W. B.; Kawara, T.; Pac, C. J. *J. Mater. Chem.* **1994**, *4*, 1571. (i) Ray, P. C.; Das, P. K. *Chem. Phys. Lett.* **1995**, *244*, 153. (j) Park, G.; Cho, B. R. *J. Phys. Org. Chem.* **2004**, *17*, 169.

(20) (a) Holst, H. C.; Pakula, T.; Meier, H. *Tetrahedron* **2004**, *60*, 6765. (b) Lee, H.; Kim, D.; Lee, H. K.; Qiu, W. F.; Oh, N. K.; Zin, W. C.; Kim, K. *Tetrahedron Lett.* **2004**, *45*, 1019. (c) Meier, H.; Holst, H. C.; Oehlhof, A. *Eur. J. Org. Chem.* **2003**, 4173. (d) Lee, C. H.; Yamamoto, T. *Bull. Chem. Soc. Jpn.* **2002**, *75*, 615. (e) Lee, C. H.; Yamamoto, T. *Tetrahedron Lett.* **2001**, *42*, 3993.

(21) Examples of luminescent coordination compounds: (a) Polson, M. I. J.; Medlycott, E. A.; Hanan, G. S.; Mikelsons, L.; Taylor, N. L.; Watanabe, M.; Tanaka, Y.; Loiseau, F.; Passalacqua, R.; Campagna, S. *Chem. Eur. J.* **2004**, *10*, 3640. (b) Liu, Q. D.; Jia, W. L.; Wu, G.; Wang, S. *Organometallics* **2003**, *22*, 3781. (c) Seward, C.; Pang, J.; Wang, S. *Eur. J. Inorg. Chem.* **2002**, 1390. (d) Ma, D. L.; Che, C. M. *Chem. Eur. J.* **2003**, *9*, 6133. (e) Wan, S. Y.; Li, Y. Z.; Okamura, T.; Fan, J.; Sun, W. Y.; Ueyama, N. *Eur. J. Inorg. Chem.* **2003**, 3783. (f) Metcalfe, C.; Spey, S.; Adams, H.; Thomas, J. A. *Dalton* **2002**, 4732.

(22) Additional examples of coordination compounds with triazine-based ligands. (a) Seward, C.; Jia, W.; Wang, R. Y.; Wang, S. *Inorg. Chem.* **2004**, *43*, 978. (b) Carrion, M. C.; Guerrero, A.; Jalon, F. A.; Manzano, B. R.; de la Hoz, A.; Claramunt, R. M.; Milata, V.; Elguero, J. *Inorg. Chem.* **2003**, *42*, 885. (c) Kusakawa, T.; Fujita, M. *J. Am. Chem. Soc.* **2002**, *124*, 13576. (d) Bosch, E.; Barnes, C. L. *Inorg. Chem.* **2002**, *41*, 2543. (e) Pike, R. D.; Borne, B. D.; Maeyer, J. T.; Rheingold, A. L. *Inorg. Chem.* **2002**, *41*, 631. (f) Biradha, K.; Fujita, M. *Angew. Chem., Int. Ed.* **2002**, *41*, 3392. (g) Henke, K. R.; Hutchison, A. R.; Krepps, M. K.; Parkin, S.; Atwood, D. A. *Inorg. Chem.* **2001**, *40*, 4443. (h) Hong, M. C.; Zhao, Y. J.; Su, W. P.; Cao, R.; Fujita, M.; Zhou, Z.; Chan, A. S. C. *Angew. Chem., Int. Ed.* **2000**, *39*, 2468. (i) Abrahams, B. F.; Batten, S. R.; Grannas, M. J.; Hamit, H.; Hoskins, B. F.; Robson, R. *Angew. Chem., Int. Ed.* **1999**, *38*, 1475.

(23) Hayami, S.; Inoue, K. *Chem. Lett.* **1999**, 545.



are related by a pseudo- C_3 rotation axis. The geometry around each ruthenium center can be described as a distorted octahedron with the alkynyl ligand trans to the chloride, as reported for other $\text{RuCl}(\text{C}\equiv\text{CR})(\text{dppe})_2$ complexes (for example, $\text{R} = \text{Ph}$, $\text{C}_6\text{H}_4\text{NO}_2$).^{25b} The $\text{Ru}-\text{C}$ and $\text{C}\equiv\text{C}$ distances are normal, compared to those in $\text{RuCl}(\text{C}\equiv\text{CR})(\text{dppe})_2$ and $\text{RuCl}(\text{C}\equiv\text{CR})(\text{dppm})_2$.^{25b,27}

Electrochemistry. The redox behavior of the trimetallic ruthenium complexes **5–7** in CH_2Cl_2 has been investigated by cyclic voltammetry with $n\text{-Bu}_4\text{PF}_6$ as the supporting electrolyte. Complexes **5–7** exhibited only one redox wave at 0.278, 0.152, and 0.369 V vs AgCl/Ag , respectively. The electrochemical behavior is similar to those of $1,3,5\text{-[CpFe}(\eta^5\text{-C}_5\text{H}_4\text{C}\equiv\text{C})\text{]}_3\text{C}_6\text{H}_3$ ²⁸ and $1,3,5\text{-[Cl(dppe)}_2\text{MC}\equiv\text{CC}_6\text{H}_4\text{C}\equiv\text{C})\text{]}_3\text{C}_6\text{H}_3$ ($\text{M} = \text{Ru}$,⁵ Os ⁸), which also only show a single redox wave. In contrast, three separated one-electron redox waves were observed in the related complexes $1,3,5\text{-[Cp(PPh}_3)_2\text{RuC}\equiv\text{C]}_3\text{C}_6\text{H}_3$ ³

Table 1. Crystal Data and Structure Refinement Details for $2,4,6\text{-[4-(Cl(dppe)}_2\text{RuC}\equiv\text{C})\text{C}_6\text{H}_4\text{]}_3\text{-1,3,5-C}_3\text{N}_3$ (5**)**

formula	$\text{C}_{183}\text{H}_{156}\text{N}_3\text{P}_{12}\text{Cl}_3\text{Ru}_3\cdot\text{C}_6\text{H}_6\cdot\text{C}_6\text{H}_{14}\cdot 5\text{CH}_2\text{Cl}_2\cdot 1.5\text{H}_2\text{O}$
formula wt	3794.24
cryst syst	triclinic
space group	$\text{P}\bar{1}$
a , Å	18.274(4)
b , Å	18.582(4)
c , Å	27.929(6)
α , deg	96.925(4)
β , deg	103.277(4)
γ , deg	90.856(4)
V , Å ³	9154(3)
Z	2
calcd density, g cm^{-3}	1.377
abs. coeff, mm^{-1}	0.593
$F(000)$	3910
θ range, deg	1.42–25.00
no. of rflns collected	67 316
no. of indep rflns	31 932 ($R(\text{int}) = 0.0969$)
no. of obsd rflns ($I > 2\sigma(I)$)	16 426
no. of data/restraints/params	31 932/33/2084
goodness of fit on F^2	0.988
final R indices ($I > 2\sigma(I)$)	$R1 = 0.0724$, $wR2 = 0.1713$
largest diff peak and hole, $\text{e}\text{\AA}^{-3}$	1.221 and -0.907

(27) Faulkner, C. W.; Ingham, S. L.; Khan, M. S.; Lewis, J.; Long, N. J.; Raithby, P. R. *J. Organomet. Chem.* **1994**, *482*, 139.

(28) Fink, H.; Long, N. J.; Martin, A. J.; Opromolla, G.; White, A. J. P.; Williams, D. J.; Zanello, P. *Organometallics* **1997**, *16*, 2646.

Table 2. Bond Lengths and Angles for 2,4,6-[4-(Cl(dppe)₂RuC≡C)C₆H₄]₃-1,3,5-C₃N₃ (5)

Bond Lengths (Å)			
Ru(1)–P(11)	2.3930(9)	Ru(1)–Cl(1)	2.4708(8)
Ru(1)–P(12)	2.3723(9)	Ru(1)–C(19)	2.000(3)
Ru(1)–P(13)	2.3479(9)	C(18)–C(19)	1.187(4)
Ru(1)–P(14)	2.3504(8)		
Ru(2)–P(21)	2.3742(10)	Ru(2)–Cl(2)	2.4956(8)
Ru(2)–P(22)	2.3568(9)	Ru(2)–C(29)	1.979(2)
Ru(2)–P(23)	2.3606(9)	C(28)–C(29)	1.181(4)
Ru(2)–P(24)	2.3737(9)		
Ru(3)–P(31)	2.3727(9)	Ru(3)–Cl(3)	2.5111(8)
Ru(3)–P(32)	2.3548(7)	Ru(3)–C(39)	1.987(2)
Ru(3)–P(33)	2.3550(9)	C(38)–C(39)	1.205(4)
Ru(3)–P(34)	2.3655(8)		
Bond Angles (deg)			
P(13)–Ru(1)–P(11)	177.56(3)	P(14)–Ru(1)–P(12)	178.04(3)
P(12)–Ru(1)–P(11)	82.69(3)	P(13)–Ru(1)–P(12)	95.29(3)
P(13)–Ru(1)–P(14)	82.77(3)	P(14)–Ru(1)–P(11)	99.25(3)
P(11)–Ru(1)–Cl(1)	79.31(3)	P(12)–Ru(1)–Cl(1)	88.56(3)
P(13)–Ru(1)–Cl(1)	102.06(3)	P(14)–Ru(1)–Cl(1)	91.57(3)
C(19)–Ru(1)–P(11)	97.03(8)	C(19)–Ru(1)–P(12)	95.63(7)
C(19)–Ru(1)–P(13)	81.77(8)	C(19)–Ru(1)–P(14)	84.39(7)
C(19)–Ru(1)–Cl(1)	174.07(8)	C(18)–C(19)–Ru(1)	172.2(2)
C(19)–C(18)–C(15)	177.8(3)		
P(23)–Ru(2)–P(21)	179.50(3)	P(22)–Ru(2)–P(24)	176.18(3)
P(22)–Ru(2)–P(21)	83.96(3)	P(22)–Ru(2)–P(23)	95.79(3)
P(23)–Ru(2)–P(24)	80.46(3)	P(24)–Ru(2)–P(21)	99.78(3)
P(21)–Ru(2)–Cl(2)	94.64(3)	P(22)–Ru(2)–Cl(2)	88.06(3)
P(23)–Ru(2)–Cl(2)	84.92(3)	P(24)–Ru(2)–Cl(2)	90.85(3)
C(29)–Ru(2)–P(21)	82.99(8)	C(29)–Ru(2)–P(22)	88.41(8)
C(29)–Ru(2)–P(23)	97.44(8)	C(29)–Ru(2)–P(24)	92.81(8)
C(29)–Ru(2)–Cl(2)	175.93(8)	C(28)–C(29)–Ru(2)	177.7(3)
C(29)–C(28)–C(25)	172.4(3)		
P(33)–Ru(3)–P(31)	177.41(3)	P(32)–Ru(3)–P(34)	172.49(3)
P(32)–Ru(3)–P(31)	82.43(3)	P(33)–Ru(3)–P(32)	96.34(3)
P(33)–Ru(3)–P(34)	82.43(3)	P(34)–Ru(3)–P(31)	98.49(3)
C(39)–Ru(3)–P(31)	86.15(8)	C(39)–Ru(3)–P(32)	82.60(7)
C(39)–Ru(3)–P(33)	91.43(8)	C(39)–Ru(3)–P(34)	90.01(7)
P(31)–Ru(3)–Cl(3)	99.32(3)	P(32)–Ru(3)–Cl(3)	101.49(3)
P(33)–Ru(3)–Cl(3)	83.15(3)	P(34)–Ru(3)–Cl(3)	85.75(3)
C(39)–Ru(3)–Cl(3)	173.51(8)	C(38)–C(39)–Ru(3)	179.7(3)
C(39)–C(38)–C(35)	177.1(3)		

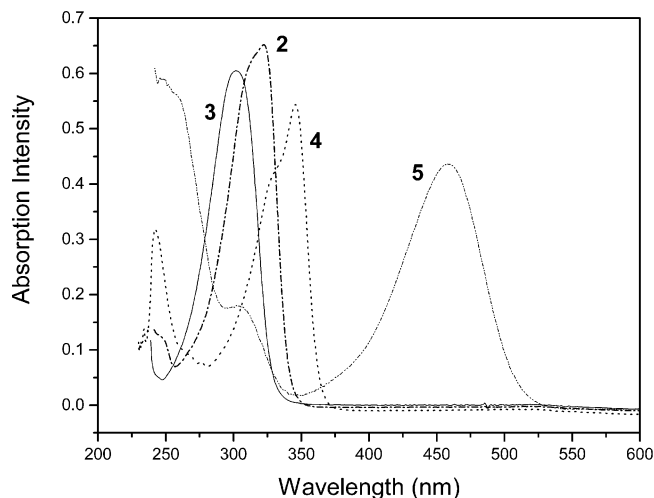
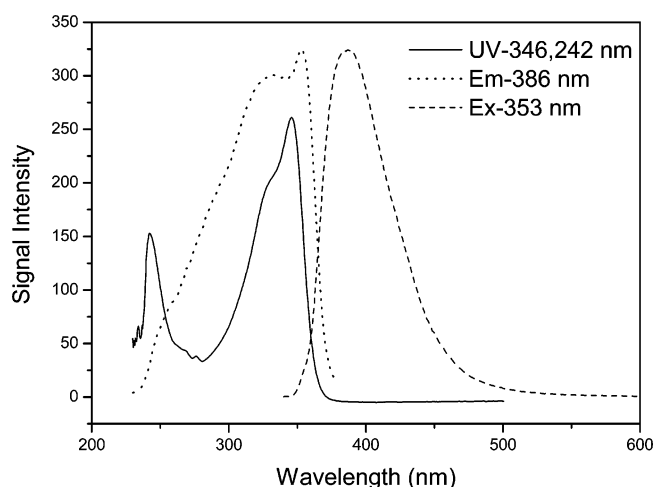
Table 3. Photophysical Data of Compounds 2–7^a

compd	λ_{\max} (nm) [ϵ (10^4 M ⁻¹ cm ⁻¹)]	β^{1064} (10^{-30} esu) ^b	β_0^c
2	323 [10.81]		
3	302 (8.43)		
4	242 [8.22], 346 [14.02]	67	35
5	302 [4.23], 459 [10.27]	457	95
6	310 [7.59], 460 [10.07]	505	106
7	314 [5.78], 472 [13.52]	558	107

^a All experiments are performed at room temperature in chloroform solution. ^b *p*-Nitroaniline (*p*NA) was used as the external reference ($\beta = 7.2 \times 10^{-30}$ esu).³⁵ The error is about $\pm 10\%$. ^c Static values of first-order hyperpolarizability (β_0) were calculated according to the three-level model.³⁶

and 1,3,5-[Cp*(dppe)FeC≡C]₃C₆H₃,^{2d} which have less extended structures.

Absorption and Emission Spectroscopy. We have investigated the absorption and emission properties of compounds 2–7, and the photophysical data of the compounds are summarized in Table 3. As illustrated in Figure 2, the UV–vis spectrum of the organic compound 2,4,6-[4-(HC≡C)C₆H₄]₃-1,3,5-C₃N₃ (**3**) in chloroform showed an intense band with λ_{\max} at 302 nm, which can be attributed to a $\pi \rightarrow \pi^*$ transition. The UV–vis spectrum of 2,4,6-[4-(Me₃SiC≡C)C₆H₄]₃-1,3,5-C₃N₃ (**2**) is similar to that of compound **3** and displayed an intense band with λ_{\max} at 323 nm. The gold acetylide

**Figure 2.** UV–vis spectra of 2–5 in CHCl₃.**Figure 3.** Absorption (—, CHCl₃, 298 K), excitation (···), and emission (---, CHCl₃, 298 K, compound concentration 2.3×10^{-6} M) spectra of **4**.

complex 2,4,6-[4-(PPh₃)AuC≡C]C₆H₄]₃-1,3,5-C₃N₃ (**4**) in chloroform showed an intense band with λ_{\max} at 346 nm, which is slightly longer than those of 2,4,6-[4-(HC≡C)-C₆H₄]₃-1,3,5-C₃N₃ (**3**; 302 nm) and 2,4,6-[4-(Me₃SiC≡C)C₆H₄]₃-1,3,5-C₃N₃ (**2**; 323 nm). The absorption spectra of the ruthenium acetylide complexes **5–7** are similar to each other and showed two intense absorption bands with λ_{\max} around 310 and 460 nm, which can be attributed to an intraligand $\pi \rightarrow \pi^*$ transition and an MLCT transition, respectively. It is noted that the $\pi \rightarrow \pi^*$ transition occurs at a wavelength similar to that of **3** (302 nm) and is shorter than those of the organic compound **2** (323 nm) and the gold acetylide complex **4** (346 nm).

We have also studied the photoluminescent properties of compounds 2–7. The organic compounds **2** and **3** and the ruthenium complexes **5–7** in chloroform solutions were found to be nonemissive or very weakly emissive, if at all. In contrast, the gold acetylide complex **4** was found to be emissive and exhibits an emission peak at 401 nm when irradiated at 353 nm (Figure 3). It is probably not surprising that the gold acetylide complex **4** is emissive while the ruthenium acetylide complexes **5–7** are not. Indeed, a number of luminescent gold(I)

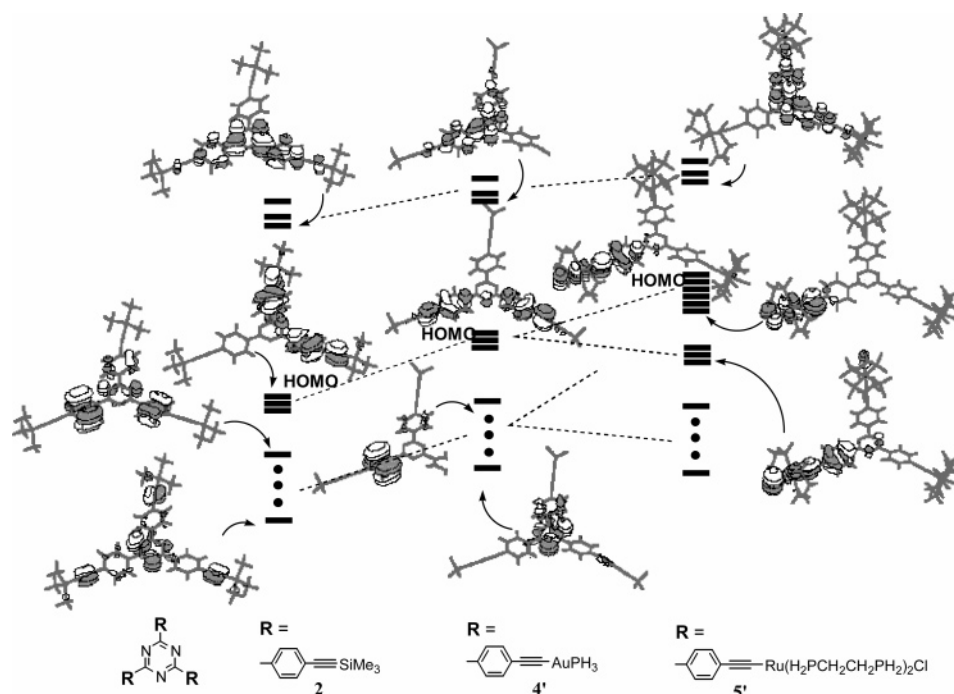


Figure 4. Orbital energy levels of **2**, **4'**, and **5'** in the frontier region. Only representative orbitals are plotted.

acetylide complexes have been reported.^{24,29} In contrast, ruthenium acetylide complexes that are luminescent at room temperature are rare.³⁰

Theoretical Study. To better understand the photophysical properties, the electronic structures of model organic and organometallic compounds have been studied by computational chemistry. In particular, it is desirable to get the following information from the study. (1) What are the origins of the electronic transitions giving the absorption bands in the UV–vis spectra? (2) How do the substituents (H, SiMe₃) and metal centers affect the electronic structures and therefore the λ_{max} values? (3) Why is the gold complex **4** emissive, while the ruthenium complexes **5**–**7** are not?

Figure 4 gives the orbital energy correlation diagram for 2,4,6-[4-(Me₃SiC≡C)C₆H₄]₃-1,3,5-C₃N₃ (**2**), 2,4,6-[(H₃P)AuC≡C]C₆H₄]-1,3,5-C₃N₃ (**4'**), and 2,4,6-[4-(Cl-(H₂PCH₂CH₂PH₂)₂RuC≡C)C₆H₄]-1,3,5-C₃N₃ (**5'**). **4'** and **5'** are models in our molecular orbital calculations for **4** and **5**, respectively. As shown in Figure 4, **2** has three highest occupied molecular orbitals (HOMOs) having similar orbital energies. These three HOMOs are formed from the linear combinations of the three highest π -bonding orbitals of the three aryl substituents at the 1-, 3-, and 5-positions of triazine. The three lowest unoccupied molecular orbitals (LUMOs) of **2** are molecular orbitals derived from the π^* orbitals of the triazine core mixed extensively with the π^* orbitals of the three aryl substituents. The π^* orbitals of the triazine core are mainly composed of the N p_{π} orbital, because N has a greater electronegativity than C. Lying below the

three HOMOs are the molecular orbitals accommodating the N lone pair electrons from the triazine core and other π -bonding electron pairs. The orbital pattern suggests that the electronic transition resulting in the absorption band at the longest wavelength (λ_{max} of 323 nm) in the electronic spectrum of **2** can be attributed to charge transfer from peripheral aryl groups to the central triazine core. When the SiMe₃ groups in **2** are replaced with H to give **3**, the electronic structure in the frontier regions does not change much, except that the HOMO–LUMO gap is slightly increased; thus, the transition gives an absorption band with a shorter λ_{max} at 302 nm.

When the SiMe₃ groups in **2** are replaced with Au(PH₃) to give **4'**, the electronic structure in the frontier regions does not change significantly, either. The gold's nonbonding d orbitals lie far below the HOMOs. The more ionic Au–C bonds in compound **4'** in comparison to the Si–C bonds in compound **2** makes the π -conjugation system more electron rich and, therefore, leads to destabilization of the HOMOs and a smaller HOMO–LUMO gap, consistent with the experimental observation that $\lambda_{\text{max}}(\mathbf{2}, 323 \text{ nm}) < \lambda_{\text{max}}(\mathbf{4}, 358 \text{ nm})$.

The LUMOs of the ruthenium complex **5'** are similar to those of **4'**. However, **5'** has six filled metal (d)-dominated molecular orbitals above the three molecular orbitals related to the HOMOs of **2**, due to the presence of the three Ru fragments. Here, each Ru fragment contributes two metal d_{π} orbitals if we define C–Ru–Cl as the σ -bonding axis. Each Ru fragment is thought to have three metal d orbitals (2 d_{π} + 1 d_{δ}): i.e., the so-called “ t_{2g} ” set of orbitals. The two d_{π} orbitals are lying higher in energy than the d_{δ} orbital, due to the presence of the π -donating chloride ligand. The three molecular orbitals related to the HOMOs of **2** are stabilized due to their π -bonding interactions with the $d_{\pi}(\text{Ru})$ orbitals, leading to a large energy gap between these orbitals and the LUMOs. The orbital patterns

(29) (a) Yip, S. K.; Cheng, E. C. C.; Yuan, L. H.; Zhu, N. Y.; Yam, V. W. W. *Angew. Chem., Int. Ed.* **2004**, *43*, 4954. (b) Cheung, K. L.; Yip, S. K.; Yam, V. W. W. *J. Organomet. Chem.* **2004**, *689*, 4451. (c) Lu, W.; Zhu, N. Y.; Che, C. M. *J. Am. Chem. Soc.* **2003**, *125*, 16081.

(30) (a) Wong, C. Y.; Chan, M. C. W.; Zhu, N. Y.; Che, C. M. *Organometallics* **2004**, *23*, 2263. (b) Adams, C. J.; Pope, S. J. A. *Inorg. Chem.* **2004**, *43*, 3492. (c) Wong, W. Y.; Ho, K. Y.; Ho, S. L.; Lin, Z. J. *Organomet. Chem.* **2003**, *683*, 341. (d) van Slageren, J.; Winter, R. F.; Klein, A.; Hartmann, S. J. *Organomet. Chem.* **2003**, *670*, 137.

shown in Figure 4 suggest that the two bands with λ_{\max} values of 302 and 459 nm in the UV-vis spectrum of **5** can be attributed to $\pi \rightarrow \pi^*$ and MLCT absorption bands, respectively. The calculation also confirms that the λ_{\max} value due to $\pi \rightarrow \pi^*$ for **5** is shorter and the λ_{\max} value due to MLCT for **5** is longer than the λ_{\max} value due to $\pi \rightarrow \pi^*$ for **4**. Apparently, replacement of Cl in **5** with acetylide ligands to give **6** and **7** does not change the orbital pattern on the frontier region. A recent study of the electronic structures of $\text{RuCl}(\text{C}\equiv\text{CPh})(\text{dppe})_2$ and $\text{Ru}(\text{C}\equiv\text{CPh})_2(\text{dppe})_2$ shows that the HOMOs and LUMOs of these simpler acetylide complexes are mostly d(Ru) in nature.³¹

Why is the gold complex **4** emissive, while the ruthenium complexes **5–7** are not? From the orbital pattern shown in Figure 4, we can see that the lowest excited state of gold complex **4'** is the $\pi \rightarrow \pi^*$ state and the lowest excited state of ruthenium complex **5'** is the MLCT state. The energy gap between the MLCT state and the ground state in **5'** is smaller than that between the $\pi \rightarrow \pi^*$ state and the ground state in **4'**. Thus, quenching to the ground state is more efficient in **5**, as expected from the energy gap law, which states that the radiationless process becomes more efficient as the emitting state approaches the ground state.³²

Hyperpolarizability. The nonlinear optical properties of octupolar molecules have been receiving increasing attention in recent years.^{33,34} The first hyperpolarizability β^{1064} values have been reported for several octupolar acetylide complexes, including 1,3,5-[Cp^{*}-(dppe)FeC≡C]₃C₆H₃,^{2a} 1,3,5-[(PPh₃)AuC≡C]₃C₆H₃,¹⁵ 1,3,5-[X(dppe)₂RuC≡CC₆H₄C≡C]₃C₆H₃ (X = Cl, C≡CPh),^{6a} and 1,3,5-[Cl(PP)₂RuC≡CC₆H₄CH=CH]₃C₆H₃ (PP = dpmp, dppe).^{7a} In this work, we have also tried to determine the first hyperpolarizability β^{1064} values of complexes **2–7** by hyper-Raleigh scattering experiments at 1064 nm. The HRS signals of **2** and **3** are weak, and the β^{1064} values could not be confidently estimated with our setup. The β^{1064} value of the gold acetylide complex **4** was determined to be 67×10^{-30} esu, using *p*-nitroaniline (*p*NA, $\beta = 7.2 \times 10^{-30}$ esu)³⁵ as the reference. The static β_0 value was calculated to be $35 \times$

10^{-30} esu, on the basis of the three-level model.³⁶ Although the ruthenium complexes were found to be nonemissive on irradiation with UV-vis light, we observed that they exhibit two-photon absorption-induced fluorescence (2PA) in the HRS experiments at 1064 nm. To estimate their β values, the contributions of 2PA to the HRS signals were removed by curve fitting.³⁷ In comparison to the gold complex **4**, the ruthenium complexes **5–7** have significantly larger β^{1064} values (**5**, 457×10^{-30} esu; **6**, 505×10^{-30} esu; **7**, 558×10^{-30} esu) or β_0 values (**5**, 95×10^{-30} esu; **6**, 106×10^{-30} esu; **7**, 107×10^{-30} esu). A similar trend has been observed previously. For example, the β^{1064} value of 1,3,5-[(PPh₃)AuC≡C]₃C₆H₃ ($\beta = 4 \times 10^{-30}$ esu)¹⁵ is also reported to be smaller than those of 1,3,5-[Cl(dppe)₂RuC≡CC₆H₄C≡C]₃C₆H₃ ($\beta = 94 \times 10^{-30}$ esu)^{6a} and 1,3,5-[Cl(dpmp)₂RuC≡CC₆H₄CH=CH]₃C₆H₃ ($\beta = 244 \times 10^{-30}$ esu).^{7a} It should be noted that these reported β values were calculated in reference to *p*NA, assuming that the β value of *p*NA is 21.4×10^{-30} esu. In our calculation, we have used a smaller β value of *p*NA (7.2×10^{-30} esu), as suggested by Wang et al.³⁵

Since the triazine core is an electron acceptor, one might expect that the first hyperpolarizabilities of triazine derivatives should increase with a stronger donor on the 2,4,6-positions. According to the electrochemical data of **5–7**, the donor strength of the (dppe)₂Ru centers is in the order of **6** > **5** > **7**. The same order in the hyperpolarizabilities is expected. Experimentally, the β_0 values of **5–7** are very close and complex **7** exhibits a second-order nonlinearity similar to that of **6** and larger than that of **5**. It is not clear to us why the trends in the electrochemical data and the hyperpolarizabilities are different. Probably, it is related to the effect of RuCl, RuC≡CC₆H₄OMe, and RuC≡CC₆H₄NO₂ on the second-order nonlinearity. We noticed that the β_0 values of RuCl(C≡CC₆H₅)(PP)₂ (PP = dpmp, dppe) are smaller than those of RuCl(C≡CC₆H₄NO₂)(PP)₂.^{17b}

Summary. Several gold and ruthenium acetylide complexes with a 1,3,5-triazine core have been synthesized. The gold acetylide complex was found to be photoluminescent, while the ruthenium complexes are not. Theoretical studies suggest that the triazine core functions as an electron acceptor in the electronic transitions. It has also been demonstrated that both the gold and ruthenium acetylide complexes exhibit second-order NLO properties with the ruthenium complexes having a higher first hyperpolarizability than the gold complex. Our experiments support the idea that the first molecular hyperpolarizabilities of triazine derivatives with donors at the 2,4,6-positions are larger than those of analogous 1,3,5-substituted benzene derivatives, as triazine is a better acceptor core. It is worthwhile to further explore the NLO properties of octupolar organometallic complexes with a 1,3,5-triazine core.

(31) Powell, C. E.; Cifuentes, M. P.; Morrall, J. P.; Stranger, R.; Humphrey, M. G.; Samoc, M.; Luther-Davies, B.; Heath, G. A. *J. Am. Chem. Soc.* **2003**, *125*, 602.

(32) Demas, J. N.; DeGraff, B. A. In *Topics in Fluorescence Spectroscopy*; Lakowicz, J. R., Ed.; Kluwer Academic: New York, 1991; Vol. 4, p 71.

(33) Zyss, J.; Ledoux, I. *Chem. Rev.* **1994**, *94*, 77.

(34) Examples of recent work: (a) Claessens, C. G.; Gonzalez-Rodriguez, D.; Torres, T.; Martin, G.; Agullo-Lopez, F.; Ledoux, I.; Zyss, J.; Ferro, V. R.; Garcia de la Vega, J. M. *J. Phys. Chem. B* **2005**, *109*, 3800. (b) Yang, S. K.; Ahn, H. C.; Jeon, S. J.; Asselberghs, I.; Clays, K.; Persoons, A.; Cho, B. R. *Chem. Phys. Lett.* **2005**, *403*, 68. (c) Xia, H. P.; Wen, T. B.; Hu, Q. Y.; Wang, X.; Chen, X. G.; Shek, L. Y.; Williams, I. D.; Wong, K. S.; Wong, G. K. L.; Jia, G. *Organometallics* **2005**, *24*, 562. (d) Viau, L.; Bidault, S.; Maury, O.; Brasselet, S.; Ledoux, I.; Zyss, J.; Ishow, E.; Nakatani, K.; Le Bozec, H. *J. Am. Chem. Soc.* **2004**, *126*, 8386. (e) Porres, L.; Mongin, O.; Katan, C.; Charlot, M.; Pons, T.; Mertz, J.; Blanchard-Desce, M. *Org. Lett.* **2004**, *6*, 47. (f) Le Floch, V.; Brasselet, S.; Zyss, J.; Cho, B. R.; Lee, S. H.; Jeon, S. J.; Cho, M.; Min, K. S.; Suh, M. P. *Adv. Mater.* **2005**, *17*, 196. (g) Maury, O.; Viau, L.; Senechal, K.; Corre, B.; Guegan, J. P.; Renouard, T.; Ledoux, I.; Zyss, J.; Le Bozec, H. *Chem. Eur. J.* **2004**, *10*, 4454. (h) Asselberghs, I.; Clays, K.; Persoons, A.; Ward, M. D.; McCleverty, J. *J. Mater. Chem.* **2004**, *14*, 2831. (i) Hennrich, G.; Asselberghs, I.; Clays, K.; Persoons, A. *J. Org. Chem.* **2004**, *69*, 5077.

(35) (a) Hsu, C. C.; Liu, S.; Wang, C. C.; Wang, J. *Chem. Phys.* **2001**, *114*, 7103. (b) Tai, O. Y. H.; Wang, C. H.; Ma, H.; Jen, A. K. Y. *J. Chem. Phys.* **2004**, *121*, 6086.

(36) Three-level model: Joffe, M.; Yaron, D.; Silbey, R. J.; Zyss, J. *J. Chem. Phys.* **1992**, *97*, 5607.

(37) (a) Song, N. W.; Kang, T. I.; Jeong, S. C.; Jeon, S. J.; Cho, B. R.; Kim, D. *Chem. Phys. Lett.* **1996**, *261*, 307. (b) Kaatz, P.; Shelton, D. P. *J. Chem. Phys.* **1996**, *105*, 3918. (c) Hsu, C. C.; Huang, T. H.; Zang, Y. L.; Lin, J. L.; Cheng, Y. Y.; Lin, J. T.; Wu, H. H.; Wang, C. H.; Kuo, C. T.; Chen, C. H. *J. Appl. Phys.* **1996**, *80*, 5996. (d) Hsu, C. C.; Shu, C. F.; Huang, T. H.; Wang, C. H.; Lin, J. L.; Wang, Y. K.; Zang, Y. L. *Chem. Phys. Lett.* **1997**, *274*, 466. (e) Song, O. K.; Woodford, J. N.; Wang, C. H. *J. Phys. Chem.* **1997**, *101*, 3222. (f) Wang, C. H.; Woodford, J. N.; Jen, A. K. Y. *Chem. Phys.* **2000**, *262*, 475.

Experimental Section

All manipulations were carried out at room temperature under a nitrogen atmosphere using standard Schlenk techniques, unless otherwise stated. Solvents were distilled under nitrogen from sodium–benzophenone (hexane, diethyl ether, THF, benzene) or calcium hydride (dichloromethane, CHCl_3). The starting materials 2,4,6-[4- BrC_6H_4]₃-1,3,5- C_3N_3 ,²³ [4-($\text{Me}_3\text{SiC}\equiv\text{C}$) C_6H_4]₃-1,3,5- C_3N_3 ,^{20d} [4-($\text{HC}\equiv\text{C}$) C_6H_4]₃-1,3,5- C_3N_3 ,^{20d} and *cis*- $\text{RuCl}_2(\text{dppe})_2$ ³⁸ were prepared by modified literature methods.

Microanalyses were performed by M-H-W Laboratories (Phoenix, AZ). ¹H, ¹³C{¹H}, and ³¹P{¹H} NMR spectra were collected on a Bruker ARX-300 spectrometer (300 MHz). ¹H and ¹³C NMR chemical shifts are referenced relative to TMS, and ³¹P NMR chemical shifts are referenced relative to 85% H_3PO_4 . The electrochemical measurements were performed with a CHI 660 potentiostat. A three-component electrochemical cell was used with a glassy-carbon electrode as the working electrode, a platinum wire as the counter electrode, and an Ag/AgCl electrode as the reference electrode. The cyclic voltammograms were collected with a scan rate of 10 mV/s in CH_2Cl_2 containing 0.10 M *n*- Bu_4NPF_6 as the supporting electrolyte. The peak potentials reported were referenced to Ag/AgCl. The ferrocene/ferrocenium redox couple was located at 0.226 V under our experimental conditions. The UV–vis spectra were recorded on a MILTON ROY Spectronic 3000 spectrophotometer with dilute CHCl_3 solutions at room temperature. The fluorescence spectra were collected on a Perkin-Elmer LS55 luminescence spectrophotometer.

2,4,6-[4-($\text{Me}_3\text{SiC}\equiv\text{C}$) C_6H_4]₃-1,3,5- C_3N_3 (2). A mixture of 2,4,6-[4- BrC_6H_4]₃-1,3,5- C_3N_3 (1; 3.00 g, 5.50 mmol), $\text{Pd}(\text{PPh}_3)_4$ (0.60 g, 0.52 mmol), CuI (0.20 g, 0.10 mmol), and (trimethylsilyl)acetylene (5.0 mL, 35 mmol) in NEt_3 (50 mL)/THF (100 mL) was stirred for 6 h. The solvents were then removed under vacuum, and the residue was extracted with Et_2O (30 mL × 4). The volume of the extract was reduced to ca. 5 mL. The mixture was then loaded on an alumina column and eluted with hexane. The solvent of the elute was evaporated to afford a white solid. Yield: 2.2 g, 67%. ¹H NMR (300 MHz, CDCl_3): δ 8.60 (d, $J(\text{HH}) = 8.1$ Hz, 6 H, C_6H_4), 7.61 (d, $J(\text{HH}) = 8.1$ Hz, 6 H, C_6H_4), 0.31 (s, 27 H, SiMe_3). ¹³C{¹H} NMR (75.5 MHz, CDCl_3): δ 171.5 (s, C_3N_3), 136.4 (s, C of C_6H_4), 132.8 (s, CH of C_6H_4), 129.4 (s, CH of C_6H_4), 128.0 (s, C of C_6H_4), 105.4 (s, C≡C), 98.1 (s, C≡C), 0.62 (s, SiMe_3). IR (KBr, cm^{-1}): $\nu(\text{C}\equiv\text{C})$ 2158. Anal. Calcd for $\text{C}_{36}\text{H}_{39}\text{N}_3\text{Si}_3$: C, 72.31; H, 6.57; N, 7.03. Found: C, 72.23; H, 6.65; N, 6.76.

2,4,6-[4-($\text{HC}\equiv\text{C}$) C_6H_4]₃-1,3,5- C_3N_3 (3). To a solution of 2,4,6-[4- $\text{Me}_3\text{SiC}\equiv\text{C}$] C_6H_4]₃-1,3,5- C_3N_3 (2; 36.0 mg, 0.060 mmol) in THF (25 mL) was added a solution of Bu_4NF (1.0 mL, 1.0 M in THF). The resulting reaction mixture was stirred for 2 h. The solvent was removed, and the residue was washed with CH_3OH (30 mL × 4) and then dried under vacuum overnight to afford a white solid. ¹H NMR (300.13 MHz, CDCl_3): δ 8.71 (d, $J(\text{HH}) = 8.1$ Hz, 6 H, C_6H_4), 7.68 (d, 6 H, $J(\text{HH}) = 8.1$ Hz, 6 H, C_6H_4), 3.28 (s, 3 H, C≡CH). ¹³C{¹H} NMR (75.5 MHz, CDCl_3): δ 175.0 (s, C_3N_3), 136.6 (s, C of C_6H_4), 133.0 (s, CH of C_6H_4), 129.6 (s, CH of C_6H_4), 127.4 (s, C of C_6H_4), 84.1 (s, C≡C), 80.6 (s, C≡C).

2,4,6-[4-($\text{P}(\text{Ph}_3)\text{C}\equiv\text{C}$) C_6H_4]₃-1,3,5- C_3N_3 (4). A mixture of 2,4,6-[4- $\text{HC}\equiv\text{C}$] C_6H_4]₃-1,3,5- C_3N_3 (3; 0.060 g, 0.156 mmol) and $\text{AuCl}(\text{PPh}_3)$ (0.233 g, 0.47 mmol) in NEt_3 (1.0 mL)/THF (10 mL) was refluxed for 3 h. The solvents were removed under vacuum, and the residue was washed with CH_3OH (20 mL × 3), followed by three recrystallizations from $\text{CH}_2\text{Cl}_2/\text{CH}_3\text{OH}$ (1:5). The solid was dried under vacuum overnight. Yield: 0.12 g, 44%. ³¹P{¹H} NMR (121.50 MHz, CD_2Cl_2): δ 41.3 (s). ¹H NMR (300 MHz, CD_2Cl_2): δ 8.63 (d, $J(\text{HH}) = 8.6$ Hz, 6H,

C_6H_4), 7.46–7.58 (m, 51 H, 6 H of C_6H_4 and 45 H of PPh_3). IR (KBr, cm^{-1}): $\nu(\text{C}\equiv\text{C})$ 2105. Anal. Calcd for $\text{C}_{81}\text{H}_{57}\text{Au}_3\text{N}_3\text{P}_3$: C, 55.40; H, 3.27; N, 2.39. Found: C, 54.81; H, 3.66; N, 2.15.

2,4,6-[4-($\text{Cl}(\text{dppe})_2\text{RuC}\equiv\text{C}$) C_6H_4]₃-1,3,5- C_3N_3 (5). A mixture of *cis*- $\text{RuCl}_2(\text{dppe})_2$ (1.50 g, 1.55 mmol) and NaPF_6 (0.27 g, 1.60 mmol) in dichloromethane (25 mL) was stirred at room temperature for 2 h. Then a solution of 2,4,6-[4-($\text{HC}\equiv\text{C}$) C_6H_4]₃-1,3,5- C_3N_3 (0.20 g, 0.43 mmol) in dichloromethane (25 mL) was slowly (over 2 h) added to the reaction mixture. After the reaction mixture was stirred overnight, NEt_3 (1.0 mL) was added and the mixture was stirred for a further 30 min. The solvents were removed under vacuum, and the residue was extracted with benzene (20 mL) and filtered through Celite. The benzene was removed, and the residue was washed with methanol (30 mL × 4). The crude product was recrystallized four times from dichloromethane/hexane (1/4) and dried under vacuum overnight to afford an orange powder. Yield: 1.35 g, 98%. ³¹P{¹H} NMR (121.50 MHz, CD_2Cl_2): δ 47.6 (s). ¹H NMR (300.13 MHz, CD_2Cl_2): δ 8.55 (d, $J(\text{HH}) = 8.4$ Hz, 6 H, C_6H_4), 7.00–7.46 (m, 120 H, PPh_2), 6.80 (d, $J(\text{HH}) = 8.4$ Hz, 6 H, C_6H_4), 2.74 (br s, 24 H, PCH_2). IR (KBr, cm^{-1}): $\nu(\text{C}\equiv\text{C})$ 2040. Anal. Calcd for $\text{C}_{183}\text{H}_{156}\text{Cl}_3\text{N}_3\text{P}_2\text{Ru}_3$: C, 69.15; H, 4.95; N, 1.32. Found: C, 69.10; H, 5.13; N, 1.35.

2,4,6-[4-($\text{MeOC}_6\text{H}_4\text{C}\equiv\text{C}$) C_6H_4]₃-1,3,5- C_3N_3 (6). A mixture of 2,4,6-[4-($\text{Cl}(\text{dppe})_2\text{RuC}\equiv\text{C}$) C_6H_4]₃-1,3,5- C_3N_3 (0.318 g, 0.10 mmol), 4-methoxyphenylacetylene (0.053 g, 0.40 mmol), NaPF_6 (0.85 g, 0.50 mmol), and NEt_3 (2.0 mL) in CH_2Cl_2 (20 mL) was stirred at room temperature overnight. The solvent was removed under vacuum, and the residue was extracted with benzene and filtered through Celite. The volume of the filtrate was reduced to ca. 5 mL. An orange precipitate was obtained after addition of hexane (20 mL) to the residue. The precipitate was recrystallized twice with $\text{CH}_2\text{Cl}_2/\text{hexane}$ (1:5) and then dried under vacuum overnight to afford an orange powder. Yield: 0.310 g, 89.5%. ³¹P{¹H} NMR (121.50 MHz, C_6D_6): δ 53.0 (s). ¹H NMR (300.13 MHz, C_6D_6): δ 9.51 (d, $J(\text{HH}) = 8.4$ Hz, 6 H, C_6H_4), 8.11 (b s, 24 H, PPh_2), 7.83 (br s, 24 H, PPh_2), 7.53 (d, $J(\text{HH}) = 8.4$ Hz, 6 H, C_6H_4), 7.28–7.15 (m, 12 H for C_6H_4 and 72 H of PPh_2), 3.68 (s, 9 H, OCH_3), 2.84 (br s, 24 H, PCH_2). IR (KBr, cm^{-1}): $\nu(\text{C}\equiv\text{C})$ 2050. Anal. Calcd for $\text{C}_{210}\text{H}_{177}\text{N}_3\text{O}_3\text{P}_2\text{Ru}_3$: C, 72.78; H, 5.15; N, 1.21. Found: C, 72.71; H, 5.32; N, 1.33.

2,4,6-[4-($\text{O}_2\text{NC}_6\text{H}_4\text{C}\equiv\text{C}$) C_6H_4]₃-1,3,5- C_3N_3 (7). The complex was obtained in a fashion similar to that for 2,4,6-[4-($\text{MeOC}_6\text{H}_4\text{C}\equiv\text{C}$) C_6H_4]₃-1,3,5- C_3N_3 as a red powder. Yield: 0.26 g, 76%. ³¹P{¹H} NMR (121.50 MHz, CD_2Cl_2): δ 51.8 (s). ¹H NMR (300.13 MHz, CD_2Cl_2): δ 9.56 (d, $J(\text{HH}) = 8.4$ Hz, 6 H, C_6H_4), 8.34 (d, $J(\text{HH}) = 8.9$ Hz, 6 H, C_6H_4), 7.96 (br s, 24 H, PPh_2), 7.75 (br s, 24 H, PPh_2), 7.64 (d, $J(\text{HH}) = 8.4$ Hz, 6 H, C_6H_4), 7.23–7.08 (m, 72 H, PPh_2), 6.96 (d, $J(\text{HH}) = 8.9$ Hz, 6 H, C_6H_4), 2.75 (br s, 24 H, PCH_2). IR (KBr, cm^{-1}): $\nu(\text{C}\equiv\text{C})$ 2050. Anal. Calcd for $\text{C}_{207}\text{H}_{168}\text{N}_6\text{O}_6\text{P}_2\text{Ru}_3$: C, 70.82; H, 4.82; N, 2.39. Found: C, 70.79; H, 4.87; N, 2.51.

Crystallographic Analysis of 5. Crystals suitable for X-ray diffraction were grown from a CH_2Cl_2 solution layered with diethyl ether. An orange single crystal with approximate dimensions $0.40 \times 0.25 \times 0.05$ mm³ was mounted on a glass fiber for the diffraction experiment. Intensity data were collected on a Bruker Apex CCD area detector at 100 K and were corrected by semiempirical methods from equivalents. The structure was solved by Patterson methods, expanded by difference Fourier syntheses, and refined by full-matrix least squares on F^2 using the Bruker SHELXTL (version 5.10) program package. All non-hydrogen atoms were refined anisotropically. The hydrogen atoms were introduced at their geometric positions and refined as riding atoms. There were several types of solvent molecules present in the structure, including benzene, *n*-hexane, and dichloromethane molecules. Some of them were found to be severely disordered. A hexane and a dichloromethane molecule are disordered into two

(38) Bautista, M. T.; Cappellani, E. P.; Drouin, S. D.; Morris, R. H.; Schweitzer, C. T.; Sella, A.; Zubkowski, J. *J. Am. Chem. Soc.* **1991**, *113*, 4876.

positions. A 60% occupancy set of the six carbon atoms C(21S)–C(26S) refined anisotropically were used to model one portion of the disorder in the hexane. Another six carbon atoms, C(31S)–C(36S), refined anisotropically with 40% occupancy comprise the second set of atoms in the hexane disorder. A similar procedure was also applied to the dichloromethane with similar disorder behavior. A 60% occupancy set of C(4S), Cl(41), and Cl(42) refined anisotropically was employed to model one portion of the disorder in the dichloromethane; another set of C(5S), Cl(51), and Cl(52) refined anisotropically with 40% occupancy comprises the second set of atoms in the dichloromethane disorder. Bond length restraints were applied to model these molecules. There are 1.5 disordered water molecules, O(1W), O(2W), and O(3W), each with 50% occupancy, which correspond to the disordered hexane with 60% occupancy. Further crystallographic details are summarized in Table 1.

Computational Details. Density functional theory calculations at the B3LYP level were performed to obtain the molecular orbitals of **2**, **3**, **4'**, and **5'**. The basis set used for C, O, N, and H atoms was 6-31G, while effective core potentials with a LanL2DZ basis set were employed for Si, Cl, P, Au, and Ru.³⁹ Polarization functions were added for silicon ($\zeta_d(\text{Si}) = 0.262$), chlorine ($\zeta_d(\text{Cl}) = 0.514$), and phosphorus ($\zeta_d(\text{P}) = 0.34$).⁴⁰ All the calculations were made with the use of Gaussian 98.⁴¹ The molecular orbitals were plotted with the Molden program.⁴² The model complex **5'** used the experimental geometry of **5** by replacing the four phenyl groups of the two dppe ligands with four hydrogens. The structures of compounds **2** and **4'** were based on the experimental geometry of **5** by replacing the Ru fragments with SiMe₃ and AuPH₃,

(39) Hay, P. J.; Wadt, W. R. *J. Chem. Phys.* **1985**, *82*, 299.

(40) Huzinaga, S. *Gaussian Basis Sets for Molecular Calculations*; Elsevier Science: Amsterdam, 1984.

(41) Frisch, M. J.; Trucks, G. W.; Schlegel, H. B.; Scuseria, G. E.; Robb, M. A.; Cheeseman, J. R.; Zakrzewski, V. G.; Montgomery, J. A., Jr.; Stratmann, R. E.; Burant, J. C.; Dapprich, S.; Millam, J. M.; Daniels, A. D.; Kudin, K. N.; Strain, M. C.; Farkas, O.; Tomasi, J.; Barone, V.; Cossi, M.; Cammi, R.; Mennucci, B.; Pomelli, C.; Adamo, C.; Clifford, S.; Ochterski, J.; Petersson, G. A.; Ayala, P. Y.; Cui, Q.; Morokuma, K.; Malick, D. K.; Rabuck, A. D.; Raghavachari, K.; Foresman, J. B.; Cioslowski, J.; Ortiz, J. V.; Stefanov, B. B.; Liu, G.; Liashenko, A.; Piskorz, P.; Komaromi, I.; Gomperts, R.; Martin, R. L.; Fox, D. J.; Keith, T.; Al-Laham, M. A.; Peng, C. Y.; Nanayakkara, A.; Gonzalez, C.; Challacombe, M.; Gill, P. M. W.; Johnson, B.; Chen, W.; Wong, M. W.; Andres, J. L.; Gonzalez, C.; Head-Gordon, M.; Replogle, E. S.; Pople, J. A. *GAUSSIAN98* (Revision A.9), Gaussian, Inc, Pittsburgh, PA, 1998.

(42) Schaftenaar, G. Molden v3.5; CAOS/CAMM Center Nijmegen, Toernooiveld, Nijmegen, The Netherlands, 1999.

respectively. The structural parameters in the C–SiMe₃ and C–AuPH₃ structural units were taken from the experimental geometries of Me₃SiC≡CSiMe₃⁴³ and Ph₃PAuC≡CAuPPh₃,⁴⁴ respectively.

HRS Experiments. A high-energy picosecond Nd:YAG laser (Continuum Leopard) provides 35 ps width pulses of 9 mW vertically polarized 1064 nm radiation at 10 Hz. The light was focused on a cylindrical cell (6 mL) containing the sample. The fundamental intensity was altered by rotation of a half-wave plate placed between crossed polarizers and measured with a photodiode. An efficient condenser system was used to collect the light scattered at the harmonic frequency (532 nm) that was detected by a photomultiplier. Discrimination of the second-harmonic light from the fundamental light was accomplished by a monochromator. Actual values of the intensities were retrieved by using fast gated integrator and boxcar averager modules. All measurements were performed in chloroform using *p*-nitroaniline ($\beta = 7.2 \times 10^{-30}$ esu) as a reference.³⁵ The intrinsic β value was obtained after removing the contribution from the multiphoton absorption-induced fluorescence that can interfere with the HRS signal.³⁷ Further details of the experimental setup, data collection, and treatment can be found elsewhere.⁴⁵ Static values of first-order hyperpolarizability (β_0) were calculated according to the three-level model.³⁶

Acknowledgment. We acknowledge financial support from the Hong Kong Research Grants Council (Grant No. HKUST6187/00P) and the University Grants Committee of Hong Kong through the Area of Excellence Scheme (AoE).

Supporting Information Available: Tables of bond distances and angles, atomic coordinates and equivalent isotropic displacement coefficients, and anisotropic displacement coefficients for 2,4,6-[4-(Cl(dppe)₂RuC≡C)-C₆H₄]₃-1,3,5-C₃N₃ (**5**); crystal data are also available as a CIF file. This material is available free of charge via the Internet at <http://pubs.acs.org>.

OM0502133

(43) Bruckman, J.; Kruger, C. *Acta Crystallogr.* **1997**, *C53*, 1845.

(44) Bruce, M. I.; Grundy, K. R.; Liddell, M. J.; Snow, M. R.; Tiekink, E. R. T. *J. Organomet. Chem.* **1988**, *344*, C49.

(45) (a) Clays, K.; Persoons, A. *Rev. Sci. Instrum.* **1992**, *63*, 3285. (b) Houbrechts, S.; Clays, K.; Persoons, A.; Pikramenou, Z.; Lehn, J. M. *Chem. Phys. Lett.* **1996**, *258*, 485.